TlF and PbO under High Pressure: Unexpected Persistence of the Stereochemically Active Electron Pair**

Ulrich Häussermann,* Pedro Berastegui,
Stefan Carlson, Julien Haines, and Jean-Michel Léger

It is well known that the post-lanthanide elements thallium and lead display the inert-pair effect, that is, they form compounds in which the oxidation state is two units lower than the corresponding group valency.[1, 2] Frequently, the inert-pair effect is associated with the occurrence of a stereochemically active lone pair which results in an irregular anion environment and low coordination numbers of the cations Tl^+ and Pb^{2+}. As a consequence, open-packed crystal structures are obtained, and it is interesting that the volume required by a lone pair is on the same order as that of an oxygen or fluorine ion.[3] The most prominent examples are the isoelectronic systems PbO and TlF, the layered structures of which are shown in Figure 1.

The room-temperature modification of PbO is red, tetragonal α-PbO (litharge),[4] in which Pb^{2+} ions are situated alternately above and below squares of oxygen ions.[5] The resulting pyramidal layers are easily related to the CsCl structure, which emerges when α-PbO is compressed along the stacking direction until the lead ions of adjacent layers become coplanar, and the Pb^{2+} ions thus form a square net with the same density than that of the O^{2-} ions (Figure 1a). At about 488 °C α-PbO transforms into yellow, orthorhombic β-PbO (massicot).[6] Somewhat unusual for a high-temperature modification, massicot is 3.4% denser than litharge. The structure consists of double layers which correspond to corrugated blocks of the rock salt structure (Figure 1b). The thickness of the blocks is smaller than their separation. Apart from the corrugation, an additional distortion of the massicot double layer with respect to an ideal block of NaCl is the zigzag chain arrangement of the anions. Due to these zigzag chains, the Pb^{2+} ions are, as in litharge, tetracoordinated by anions, although in a folded-square manner.

The ground-state structure of TlF is TlF-II.[7] The structure of TlF-II was only recently unambigously resolved by neutron diffraction, and it was found to be isotypic to β-PbO (Figure 1c).[8] However, there are some delicate differences between the two structures: first, in TlF-II the thickness of the corrugated double layers is slightly larger than their separation, and second the zigzag chain arrangement of the anions within the layers is less pronounced than in massicot. Consequently, the TlF double layers are less distorted with respect to an ideal block of rock salt, and the Tl^+ ions are thus almost fivefold coordinated (4+1) by fluorine anions. At 62 °C TlF-II transforms into tetragonal TlF-I, in which the anion chains within the corrugated blocks are linear and Tl^+ is truly five-coordinate (Figure 1d).[8]

The occurrence of these open-packed structures constructed from ions is fascinating and immediately raises the question of their stability. Compared to the high-symmetry

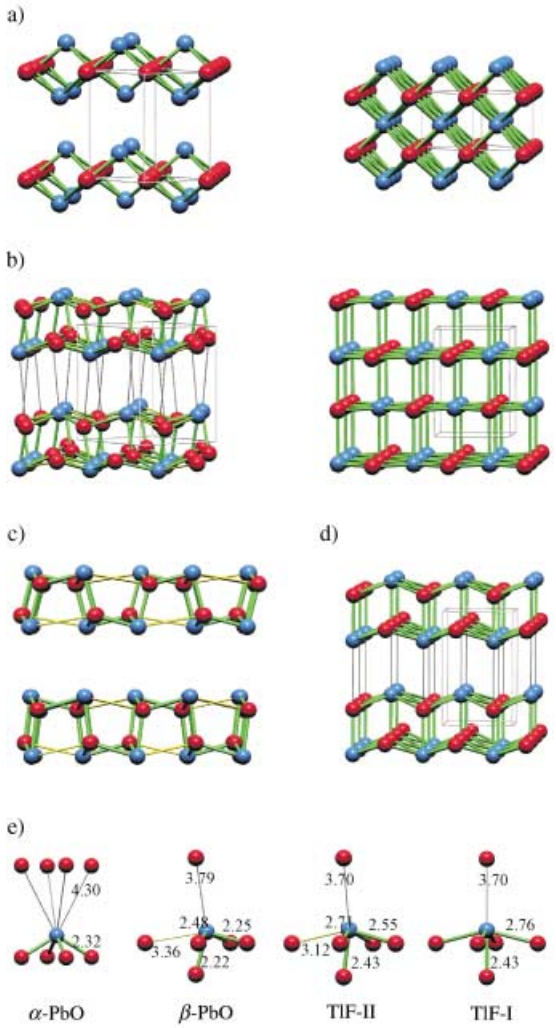

Figure 1. Structures of PbO and TlF. Cations: blue, anions: red. Nearest-neighbor cation – anion contacts are displayed as green (shortest distances), yellow (medium distances), and gray (longest distances) lines. a) The tetragonal α-PbO structure (*P*4/*nmm*) along [110] (left) and its relation to the CsCl structure (right). b) The orthorhombic β-PbO structure (*Pbcm*) approximately along [011] (left) and its relation to the NaCl structure (right). c) Comparison of the double layers (projected along [001]) in the β-PbO (top) and TlF-II structure (bottom). d) The tetragonal TlF-I structure (*P*4/*nmm*) along [100]. e) Cation coordination occurring in these open-packed lone-pair structures. The distances are in Å.

[*] Dr. U. Häussermann, Dr. P. Berastegui
Department of Inorganic Chemistry
Stockholm University
10691 Stockholm (Sweden)
Fax: (+46) 8-152187
E-mail: ulrich@inorg.su.se

Dr. S. Carlson
MAX-laboratory, Lund University
P.O. Box 118, 22643 Lund (Sweden)

Dr. J. Haines
Laboratoire de Physico-Chimie de la Matière Condensée
UMR CNRS 5617
Université Montpellier II, 34095 Montpellier (France)

Dr. J.-M. Léger
Laboratoire des Propriétés Mécaniques et Thermodynamiques des Matériaux
CNRS UPR 9001
Université Paris Nord, Villetaneuse (France)

[**] This work was supported by the Swedish National Science Research Council (NFR) and the Göran Gustafsson Foundation.

  1433-7851/01/4024-4624 $ 17.50+.50/0

structures of NaCl and CsCl, lone-pair structures are clearly unfavorable from an electrostatic point of view. This is firstly manifested in the temperature polymorphism of PbO and TlF, which indicates the presence of competing, energetically close lying, solutions to the ground-state structure, and secondly by the fact that the lone-pair structure is absent in PbS and TlCl, which adopt undistorted NaCl and CsCl structures, respectively. Therefore, under external pressure the open-packed PbO and TlF lone-pair structures might be expected to transform readily into the six-coordinate NaCl or the eight-coordinate CsCl structure. However, recent experiments at relatively low pressures (3.5 and 10.1 GPa for TlF and PbO, respectively)[8, 9] did not reveal such a structural transition. Here we present a structural investigation of TlF and PbO under much higher pressures, with rather surprising results. Additionally, the high-pressure behavior of the two systems was modeled by ab initio calculations. From the theoretical results we were able to extract a simple bonding picture for lone-pair structures involving inert-pair elements. This bonding picture accounts for the occurrence of open-packed ionically bonded structures and their stability relative to "regular" saltlike AB compounds. This issue is of fundamental significance to general chemistry.

The high-pressure structural behavior of TlF and PbO was studied at room temperature in diamond anvil cells (see Methods). The results are displayed in Figure 2. For TlF no structural change is observed, and the TlF-II ground-state structure remains stable up to the highest pressure applied (40 GPa). At this pressure the volume of TlF has dropped to less than 65 % of the ground-state volume V_0 (Figure 2a). The high compressibility of TlF-II, which is reflected in the low bulk modulus (16.0(6) GPa), is typical of layered structures. However, the compressibility along the *a* axis, that is, the stacking direction of the double layers, is lower than those along the *b* and *c* axes, which decrease by approximately the same amount with increasing pressure. The effect of pressure on the structure of TlF-II is minor: relative to the ground-state structure, at a compression of $V/V_0 = 0.65$ the double-layer building blocks are moved closer together, and the longest of the five nearest Tl^+–F^- distances has basically become equal to the four shorter ones to give five-coordinate Tl^+ ions.[10]

The high-pressure behavior of PbO is more complicated (Figure 2b). At 0.9 GPa ground-state litharge transformed into γ-PbO, an orthorhombically distorted variant of tetragonal α-PbO. Massicot was obtained gradually above 3 GPa, and this structure was maintained up to the highest pressure applied (46 GPa). The pressure-induced transition γ-PbO $\rightarrow \beta$-PbO is irreversible, and massicot is retained on decompressing to ambient conditions. The compressibility of massicot (bulk modulus 31(1) GPa) is lower than that of TlF-II. The variation of the lattice parameters under compression (larger decrease in *b* than in *a* and *c*) is interesting, because it indicates that β-PbO develops gradually into the TlF-II structure, whereby the coordination number of Pb^{2+} increases from four to five.[10] Figure 3 summarizes the structural behavior of the investigated systems at high pressure and room temperature.

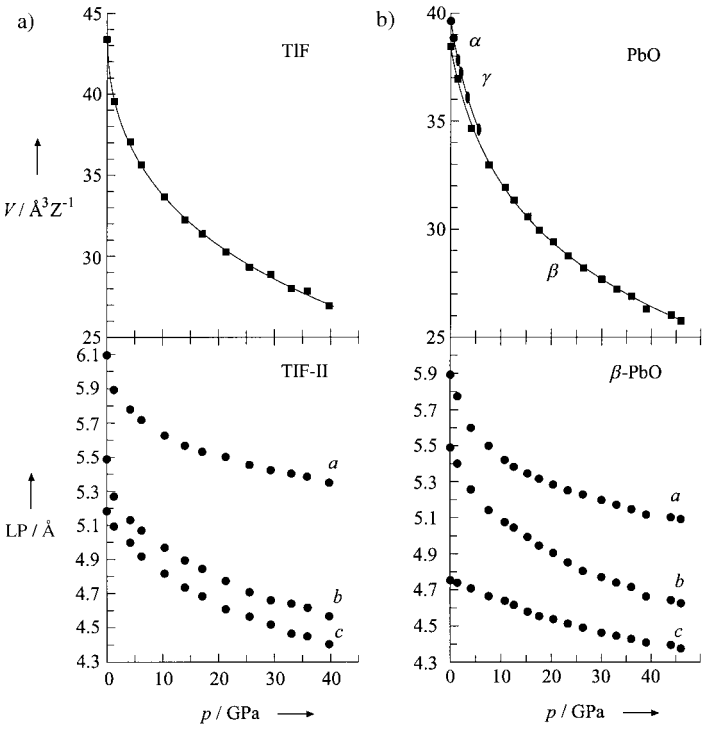

Figure 2. a) Compressibility (top) and evolution of the lattice parameters with pressure (bottom) for TlF-II (space group *Pbcm*). b) Compressibility of PbO (circles: α-PbO, ellipsoids: γ-PbO, squares: β-PbO; top) and evolution of the lattice parameters (LP) with pressure for β-PbO (space group *Pbcm*; bottom).

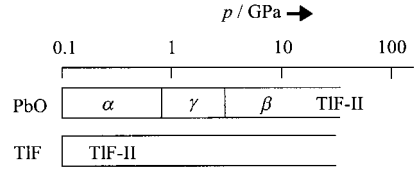

Figure 3. High-pressure structural behavior of PbO and TlF at room temperature.

In conclusion, we observe a remarkable persistence of the low-symmetry lone-pair structures β-PbO and TlF-II at high pressure. It appears surprising that these structures do not transform into the high-symmetry NaCl structure (note the close relationship of β-PbO and TlF-II to this structure) or the more densely packed CsCl structure, because the high-symmetry structures have considerably larger Madelung constants *M* and are thus clearly favored from an electrostatic viewpoint. With increasing pressure this situation becomes rapidly more pronounced, since the difference in electrostatic energy varies approximately as $\Delta M/(V/V_0)^{1/3}$. To solve this puzzle the high-pressure behavior of the systems TlF and PbO was modeled by density functional calculations by employing pseudopotentials and a plane-wave basis set.

We calculated the total energy of TlF and PbO in the structure types α-PbO, β-PbO/TlF-II, TlF-I, CsCl, and NaCl as a function of volume, including a complete relaxation of the open-packed lone-pair structures (see Methods). The results are depicted in Figure 4. We first focus on the structural competition in the low-pressure region ($0.8 < V/V_0 < 1$). For

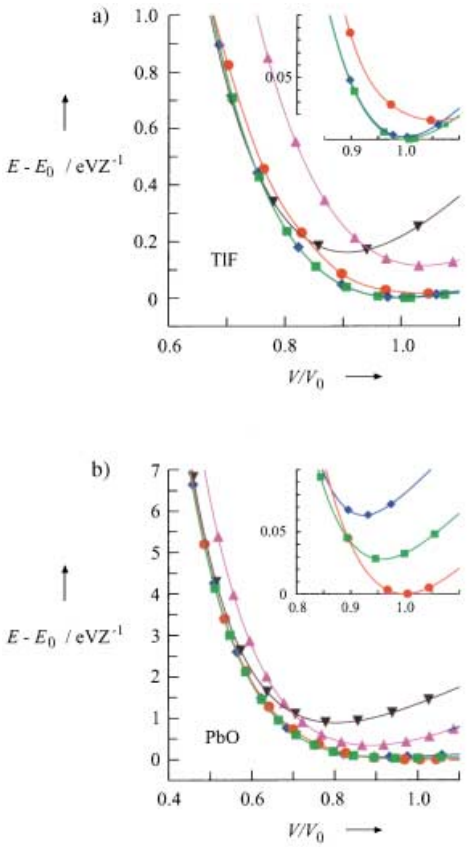

Figure 4. Calculated energy versus volume for TlF (a) and PbO (b) in the structures α-PbO (red circles), β-PbO/TlF-II (green squares), TlF-I (blue diamonds), CsCl (black triangles), and NaCl (pink triangles). E_0 is the energy of the ground state. The insets present a close up of the low-compression region.

both systems the ground-state structures are obtained correctly, although the calculated energy difference between TlF-II and TlF-I is extremely small (about 3 meV Z^{-1}) and virtually disappears under slight compression. For PbO below $V/V_0 = 0.9$ the litharge structure becomes less stable than the massicot structure (the γ modification was not considered in the calculations), and the calculated transition pressure for a direct transformation α-PbO $\rightarrow\beta$-PbO is 3.3 GPa (referring to 0 K).

In the high-compression region of this system, the β-PbO structure remains the most stable down to at least $V/V_0 \approx 0.45$ (corresponding to an external pressure of more than 150 GPa).[11] For the TlF system, however, below $V/V_0 \approx 0.75$ our calculations show the CsCl structure to be more stable than the TlF-II structure, and the transition pressure is about 20 GPa. This is in contradiction with the experimental findings, and the reason for this discrepancy is not yet resolved.[12]

In spite of this, the theoretical calculations confirm the remarkable high-pressure stability of the low-symmetry lone-pair structures and offer the possiblity of explaining their high-pressure persistence by analyzing the electronic structure. For that purpose, the density of states (DOS) of TlF in the TlF-II and CsCl structures and of PbO in the β-PbO and CsCl structures at $V/V_0 = 1$ and $V/V_0 = 0.65$ (corresponding approximately to the effect of the maximum experimental pressure) are depicted in Figure 5.

For the ground-state volume, the DOS curves for both TlF structures display a peculiar three-peak structure of the bands below the Fermi level (labeled A, B, and C in Figure 5a, left). For the PbO structures the DOS has a similar overall shape, although peaks B and C appear to have merged (Figure 5b, left), and the dispersion of the bands is generally larger than for TlF. The band gaps obtained for open-packed TlF-II and β-PbO (2.5 and 2.0 eV, respectively)[13] are considerably larger than those of TlF and PbO in the hypothetical CsCl structure (1.5 and 0.5 eV, respectively).

Under pressure (Figure 5, right) the dispersion of the bands increases, but the threefold partitioning of the DOS is still

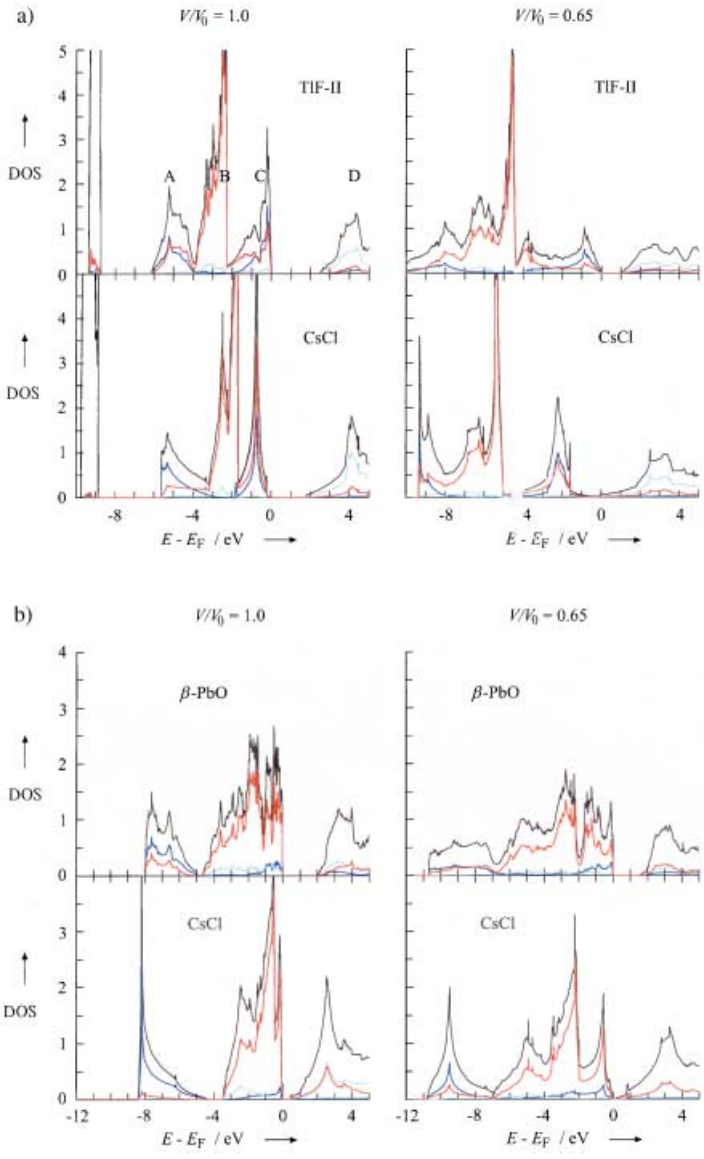

Figure 5. DOS [states/eV Z^{-1}] at the ground-state volume $V/V_0 = 1$ (left) and at a compression of $V/V_0 = 0.65$ (right) for a) TlF in the TlF-II (top) and the CsCl structure (bottom) and b) PbO in the β-PbO (top) and the CsCl structure (bottom). The letters A, B, C, and D in (a) label the different parts of the DOS as discussed in the text. Black lines: total DOS, dark blue lines: cation 6s projected DOS (pDOS), light blue lines: 6p pDOS, red lines: anion 2p pDOS.

  1433-7851/01/4024-4626 $ 17.50+.50/0

recognizable at $V/V_0 = 0.65$. Furthermore, at this compression the band gaps of TlF-II and β-PbO are diminished or have even become closed for TlF and PbO in the CsCl structure (i.e., TlF and PbO would have become metallic if the CsCl structure were attained).

We then tried to understand the characteristic shape of the DOS of these compounds and develop a simple bonding picture for open-packed structures involving inert-pair elements. The buildup of the DOS of TlF and PbO in a high-symmetry structure (NaCl or CsCl) at the ground-state volume is outlined in Figure 6. The inert-pair cations have

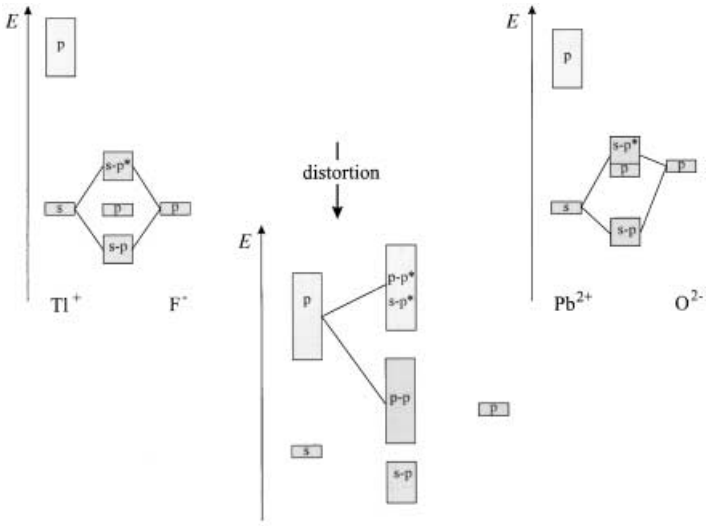

Figure 6. Schematic construction of the DOS of TlF (left) and PbO (right) in a hypothetical high-symmetry structure. Occupied bands are shaded gray. Upon distortion 6p-6s/2p mixing becomes effective, which firstly introduces some p-p bonding between cations and anions and secondly moves partly antibonding s-p states above the Fermi level. Note that in the scheme the consequences of 6p-6s/2p mixing are exaggerated.

the electron configuration $6s^2$, and the separation between the occupied 6s and empty 6p valence states is large.[14] The anions have the valence electron configuration $2p^6$. If we assume that for TlF the energies of the F^- 2p and the Tl^+ 6s states are about the same, the characteristic threefold partitioning of the bands below the Fermi level is a consequence of a strong bonding–antibonding splitting (peak A: 6s-2p bonding, peak B: 2p nonbonding, peak C: 6s-2p antibonding). Additionally the interaction between diffuse 6p orbitals gives rise to an empty band above the Fermi level.

These simple considerations reproduce the calculated DOS curve for TlF in the CsCl structure, as shown in Figure 5, very well, especially with regard to the distribution of the 6s and 2p projected DOS. Analogously, for PbO we obtain a model DOS that fits the calculated DOS under the assumption that the O^{2-} 2p states are somewhat higher in energy than the Pb^{2+} 6s states. Importantly, the closed-shell orbital interactions in TlF and PbO that yield the three-peak pattern of the DOS do not provide any bonding effect, but are instead repulsive. In other words, the ambivalent bonding situation in TlF and PbO involves attractive electrostatic interactions and effective repulsive orbital interactions, and distortion to a low-symmetry structure consequently takes place. The distortion partly removes the repulsive orbital interactions. Empty cation 6p states become available for bonding to a much greater extent than in a high-symmetry structure, because lowering of the symmetry enables 6s- and 2p-based bands to mix (hybridize) over a much larger portion of the Brillouin zone. Additionally, the energetical mismatch between the empty 6p band and the 6s/2p-based bands is diminished because the dispersion of all bands becomes larger when some ions move closer to each other in the distorted structure. The admixture of cation 6p states takes place in peaks B (nonbonding 2p bands become partly bonding) and C (partial release of 6s-2p antibonding states above the Fermi level into peak D) of the DOS.

A consequence of the latter interaction is the stabilization of states below the Fermi level, which leads to an increase in the band gap relative to the high-symmetry structure. The ratio between the number of occupied 6p and 6s states (N_p/N_s, ratio between the integrated 6p and 6s projected DOS up to the Fermi level) provides a "measure of relief" from the $6s^2$-$2p^6$ closed-shell repulsion. Figure 7 shows the N_p/N_s ratios for

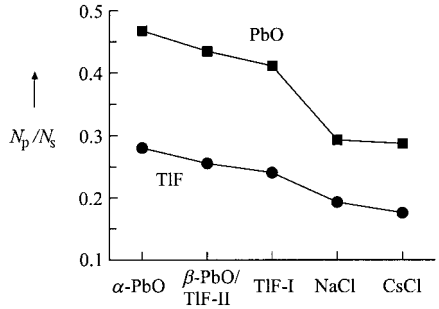

Figure 7. N_p/N_s ratios for TlF and PbO in different structures at the ground-state volume.

TlF and PbO in the considered structures at the ground-state volume. As expected, the more open packed the structure the higher the attained N_p/N_s ratio. Since the relief from the closed-shell repulsion (distortion) is at the cost of less favorable electrostatic interactions, the degree of distortion is a consequence of the balance between the contribution of electrostatic and orbital interactions to the total bonding. The ratio of the two contributions is not changed much under high pressure, because the increasingly unfavorable electrostatic interaction in the open-packed structure is countered by the stabilizing 6p-6s/2p mixing due to the larger band dispersions, which also increase. For PbO the 6p-6s/2s mixing is generally more effective than for TlF because the cation 6p states are closer in energy to the anion 2p state and, in addition, the higher ionic charges imply stronger interactions and hence larger band widths (cf. Figure 5). The apparent contradiction that the formation of a stereochemically active inert lone pair actually requires that the corresponding cation s state is active for bonding was already noted earlier for the PbO system.[15]

In conclusion, the occurrence of a stereochemically active lone pair in crystal structures with inert-pair ions is a consequence of the improvement of an unfavorable bonding situation caused by effective closed-shell repulsion ns^2-np^6. Compounds that crystallize in low-symmetry lone-pair struc-

  1433-7851/01/4024-4627 $ 17.50+.50/0

tures are not particularly stable. This is reflected in the low melting points of TlF and PbO (322 and 897 °C, respectively)[16] compared to RbF and SrO (795 and 2665 °C, respectively).[16] The cation sizes within the pairs Tl^+/Rb^+ and Pb^{2+}/Sr^{2+} are very similar, but RbF and SrO crystallize in a high-symmetry structure (NaCl), and bonding is predominantly based on electrostatic interactions. Additionally, TlF and PbO have lower melting points than TlCl and PbS (431 and 1470 °C, respectively),[16] which adopt high-symmetry structures. This is opposite to the well-known trend observed for "regular" saltlike AB compounds (i.e., alkali metal halides and alkaline earth metal chalcogenides), for which the fluorides and oxides have higher melting points than the chlorides and sulfides. The occurrence of a stereochemically active lone pair in crystal structures with inert-pair ions is decisively dependent on the relative energies of the ionic valence levels. Open-packed lone-pair structures are preferably found for fluorides and oxides because the low-lying anionic 2p states make the closed-shell $n s^2$-$n p^6$ repulsion most effective. For TlCl and PbS, in which the 3p states of the anions are comparably higher in energy, the high-symmetry CsCl and NaCl structures, respectively, are obtained.

Methods

PbO was prepared by dehydration of lead hydroxide in hot 15 N KOH.[9, 17] The powdered α-PbO was mixed with silicone grease as a pressure-transmitting medium and placed in a stainless steel gasket, preindented to a thickness of 120 μm with a 150 μm diameter hole, along with a small amount of ruby powder between the anvils of a diamond anvil cell (DAC). Pressure measurements were based on the shifts of the ruby R_1 and R_2 fluorescence lines.[18] Angle-dispersive X-ray diffraction patterns were obtained at room temperature on an imaging plate placed at between 113.65 and 117.18 mm from the sample by using Zr-filtered Mo radiation from a microfocus tube. A capillary optic was used to obtain a 100 μm diameter beam. Exposure times were typically between 24 and 60 h. The observed intensities on the imaging plates were integrated as a function of 2θ to give conventional one-dimensional diffraction profiles. The individual diffraction peaks were fitted to pseudo-Voigt functions, and the peak positions obtained were used for unit cell refinements with the program U-fit.[19]

A dried powdered sample of TlF of purity >99 % (Alfa Chemicals Ltd.) was loaded with Ar as a pressure-transmitting medium and small ruby crystals (1–2 μm diameter spheres) in a membrane-driven DAC.[20] A preindented stainless-steel gasket with a hole of 125 μm diameter and 30 μm thickness was used. The diffraction experiments were carried out at room temperature at the high-pressure dedicated beamline ID30, European Synchrotron Radiation Facility (ESFR), Grenoble, France. X rays were monochromatized to $\lambda = 0.3738(1)$ Å and the beam was focused to 0.02×0.03 mm^2 spot size at the sample position. The powder diffraction rings were collected with an on-line imaging plate detector.[21] A diffraction pattern of Si was used to determine the sample-to-detector distance (310.042 mm). Corrections for spatial distortion, calculation of imaging plate pixel size (0.07×0.08 mm^2), and subsequent integration over the complete powder rings were performed with the software FIT2D.[22] Unit cell parameters were obtained by indexing and least-square refinement with the program DICVOL91.[23]

Total energy calculations were performed within ab inito density functional theory as implemented in the program VASP.[24] Ultrasoft Vanderbilt-type pseudopotentials[25] were employed, and 5d, 6s, and 6p electrons were considered as valence electrons for Tl and Pb, and 2s and 2p electrons for F and O. The atomic position parameters and lattice parameters of the structure types α-PbO, β-PbO/TlF-II, and TlF-I were relaxed for a set of constant volumes until forces had converged to less than 0.01 eV Å^{-1}. In a second step, we extracted the equilibrium volume V_0 and the ground-state energy E_0 by fitting the E versus V values with a Birch–Murnaghan equation of state. The exchange and correlation energy was assessed by the local-density approximation (LDA).[26] Convergency of the calculations was carefully checked with respect to the plane-wave cutoff and the number of k points used in the summation over the Brillouin zone. A (high) energy value of 500 eV was chosen for the plane-wave cutoff for both systems. The k points were generated by the Monkhorst–Pack method[27] and sampled on grids of $4 \times 4 \times 4$ ($Z = 4$ structures: β-PbO, TlF-II), $6 \times 6 \times 6$ ($Z = 2$ structures: α-PbO, TlF-I), and $8 \times 8 \times 8$ ($Z = 1$ structures: CsCl, NaCl). The integration over the Brillouin zone was performed by the improved tetrahedron method.[28]

Received: June 25, 2001 [Z17348]

[1] N. V. Sidgwick, H. M. Powell, *Proc. R. Soc. London Ser. A* **1940**, *176*, 153.

[2] N. N. Greenwood, A. Earnshaw, *Chemistry of the Elements*, Pergamon, Oxford, **1997**.

[3] J. Galy, G. Meunier, S. Andersson, A. Åström, *J. Solid State Chem.* **1975**, *13*, 142.

[4] Below −85 °C α-PbO transforms into incommensurate α'-PbO (J. Moreau, J. M. Kiat, P. Garnier, G. Calvarin, *Phys. Rev. B* **1989**, *39*, 10296).

[5] J. Leciejewicz, *Acta Crystallogr.* **1961**, *14*, 1304.

[6] a) W. B. White, F. Dachille, R. Roy, *J. Am. Ceram. Soc.* **1961**, *44*, 170; b) R. J. Hill, *Acta Crystallogr. Sect. C* **1985**, *41*, 1281.

[7] C. W. F. T. Pistorius, J. B. Clark, *Phys. Rev.* **1968**, *173*, 692.

[8] P. Berastegui, S. Hull, *J. Solid State Chem.* **2000**, *150*, 266.

[9] D. M. Adams, A. G. Christy, J. Haines, S. M. Clark, *Phys. Rev. B* **1992**, *46*, 11358.

[10] The structures of TlF and PbO at the highest applied pressure could not be refined properly due to the extremely low relative X-ray scattering factor of the anions. Instead, the computationally relaxed structures TlF-II and β-PbO at $V/V_0 = 0.65$ can be used to obtain some information on the structural changes with respect to the ground-state volume. The normalized Tl–F nearest-neighbor distance distribution in TlF-II is: $V/V_0 = 1$: 1.0, 1.023, 1.078 (×2), 1.262, 1.444 (exp: 1.0, 1.044, 1.116 (×2), 1.282, 1.521); $V/V_0 = 0.65$: 1.0, 1.026, 1.065 (×2), 1.130, 1.354. The normalized Pb–O nearest-neighbor distance distribution in β-PbO is: $V/V_0 = 1$: 1.0, 1.012, 1.099 (×2), 1.528, 1.730 (exp: 1.0, 1.013, 1.117 (×2), 1.512, 1.706); $V/V_0 = 0.65$: 1.0, 1.042, 1.079 (×2), 1.138, 1.382.

[11] Above this compression the applied pseudopotentials become unreliable (see Methods).

[12] In contrast to the system PbO, for which calculated and experimental results are in excellent agreement, we observe several deviations for TlF. Apart from the calculated high-pressure transition to the CsCl structure, which is not observed experimentally, these are: 1) the calculated energy difference between the low- (TlF-II) and high-temperature modification (TlF-I) at the ground-state volume is too low; 2) the difference between the calculated and the experimental ground-state volume is considerably higher for TlF (the calculated value is about 8 % too low) than for PbO (the calculated value is about 3 % too low); 3) the relaxed structural parameters for TlF-II at the ground-state volume agree considerably less with experiment than those obtained for β-PbO (cf ref. [10]). The treatment of the exchange–correlation potential with the more advanced generalized gradient approximation (GGA) does not lead to any improvement in the results for TlF. Also, the shortcomings cannot be attributed to the applied method of calculation based on pseudopotentials and a plane-wave basis set, since full-potential techniques give virtually the same structural energy differences for TlF. Finally, one might consider neglected spin–orbit coupling as being responsible for the poorer description of TlF. However, if spin–orbit coupling affected structural stability, this should have been recognized in the PbO system as well. Hence, the discrepancies between theoretical and experimental results for TlF point to an insufficient description of this system by density functional theory, and better agreement may be obtained by a Hartree–Fock-based code. This is currently under investigation.

[13] The band gaps of TlF-II (white) and β-PbO (yellow) are underestimated by about 30 %. The underestimation of band gaps is typical of density functional calculations.

  1433-7851/01/4024-4628 $ 17.50+.50/0

[14] The already large 6s-6p separation in the atoms Tl and Pb is enhanced in the corresponding cations.
[15] a) H. J. Terpstra, R. A. de Groot, C. Haas, *Phys. Rev. B* **1995**, *52*, 11690; b) G. W. Watson, S. C. Parker, G. Kresse, *Phys. Rev. B* **1999**, *59*, 8481.
[16] A. F. Holleman, N. Wiberg, *Lehrbuch der Anorganischen Chemie*, de Gruyter, Berlin, **1995**.
[17] J. R. Schoonover, T. L. Groy, S. H. Lin, *J. Solid State Chem.* **1989**, *83*, 207.
[18] H. K. Mao, J. Xu, P. M. Bell, *J. Geophys. Res.* **1986**, *91B*, 4673.
[19] M. Evain, *U-Fit: a Cell Parameter Refinement Program*, Institut de Matériaux de Nantes, Nantes, France, **1992**.
[20] R. Letoullec, J. P. Pinceaux, P. Loubeyre, *High Pressure Res.* **1988**, *1*, 77.
[21] M. Thoms, S. Bachau, D. Häusermann, M. Kunz, T. Le Bihan, M. Mezouar, D. Strawbridge, *Nucl. Instrum. Methods Phys. Res. Sect. A* **1998**, *413*, 175.
[22] A. Hammersley, *FIT2D V10.3 Reference Manual V4.0* ESFR, Grenoble, France, **1998**.
[23] A. Boultif, D. Louër, *J. Appl. Crystallogr.* **1991**, *24*, 987.
[24] a) G. Kresse, J. Hafner, *Phys. Rev. B* **1993**, *47*, RC558; b) G. Kresse, J. Furthmüller, *Phys. Rev. B* **1996**, *54*, 11169.
[25] a) D. Vanderbilt, *Phys. Rev. B* **1990**, *41*, 7892; b) G. Kresse, J. Hafner, *J. Phys. Condens. Matter* **1994**, *6*, 8245.
[26] J. Perdew, A. Zunger, *Phys. Rev. B* **1981**, *23*, 5048.
[27] H. J. Monkhurst, J. D. Pack, *Phys. Rev. B* **1976**, *13*, 5188.
[28] P. Blöchl, O. Jepsen, O. K. Andersen, *Phys. Rev. B* **1994**, *49*, 16223.

Solid-Phase Synthesis of Transition Metal Linked, Branched Oligonucleotides**

Ignacio Vargas-Baca, Debbie Mitra, Holly J. Zulyniak, Jay Banerjee, and Hanadi F. Sleiman*

Branched oligonucleotides have recently emerged as attractive synthetic targets for the selective recognition of nucleic acids.[1] These molecules have the potential to act as sensitive diagnostic tools for the detection of DNA sequences,[1a,b] and can specifically bind single-stranded DNA/RNA (antisense/antigene strategy).[1c–e] In addition, they can serve as model complexes for the elucidation of the structure and biological role of branched RNA molecules found in nature.[1a,d] In previous branched systems, the DNA strands were linked together through oligonucleotide or small organic-molecule-based vertices.[1, 2] We recently initiated research into the synthesis and properties of a new class of branched oligonucleotides, in which a transition metal acts as the vertex joining two parallel DNA strands. Transition metal centers come in a range of geometries, coordination numbers, and bond angles that are unavailable in carbon chemistry (e.g., octahedral, square planar, trigonal bipyramidal). By combining this varied coordination chemistry with the highly specific interactions of DNA, we expect that these branched metal–DNA complexes will expand the repertoire of DNA structures to novel motifs.[3] This can be achieved both through their binding to single-stranded DNA and RNA, as well as their self-association and formation of DNA "nanostructures".[2] In addition, the rich redox and luminescence properties of metal centers afford a sensitive marker for detecting and monitoring the association of these new structures.

While many transition metal labeled oligonucleotides were reported recently,[4] the metal center is usually tethered as a pendant functional group on a DNA strand, and hence its geometry cannot influence DNA association.[5] Here we report the first synthesis of a transition metal linked branched oligonucleotide (**1**), in which the DNA strands run parallel to each other and the geometry of the metal center can directly influence the orientation of these strands. Furthermore, we have studied the biological behavior of these branched complexes by hybridization to complementary DNA. Thermal denaturation experiments show the formation of novel transition metal linked DNA duplexes with a stability comparable to that of Watson–Crick A/T duplexes.

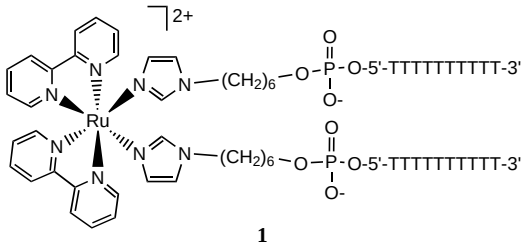

1

In the design of complex **1**, two parallel (5′-3′) oligonucleotide strands are linked to a *cis*-$[(bpy)_2Ru(imidazole)_2]^{2+}$ moiety through *n*-hexyl spacers (bpy = 2,2′-bipyridine). The ruthenium moiety is both redox active and intensely luminescent, and it has been extensively used as a probe of electron transfer processes in proteins.[6] Our convergent solid-phase strategy[7] for the preparation of ruthenium-linked parallel oligonucleotides is outlined in Schemes 1 and 2. This strategy starts with the generation of a ruthenium bis-phosphoramidite branching complex **3**.[8] The reaction of two molar equivalents of 1-(6-hydroxyhexyl)imidazole[9a] with *cis*-$[(bpy)_2Ru(CH_3CN)_2](PF_6)_2$[9b] in refluxing ethanol/water, followed by precipitation with aqueous NH_4PF_6 results in the formation of the *cis*-bis-imidazole ruthenium complex **2** as a deep red solid.[17] The UV/Vis absorption spectrum of **2** shows metal-to-ligand (Ru → bpy) charge transfer (MLCT) bands at 341 and 491 nm.[6a] An interesting feature of this complex is its intense fluorescence, which could prove useful for possible applications as a DNA biosensor. Excitation of the MLCT

[*] Prof. H. F. Sleiman, Dr. I. Vargas-Baca,[+] D. Mitra, H. J. Zulyniak, J. Banerjee
Department of Chemistry, McGill University
801 Sherbrooke St. W., Montreal, Quebec H3A 2K6 (Canada)
Fax: (+1) 514-398-3797
E-mail: hanadi.sleiman@mcgill.ca
[+] Current address:
Department of Chemistry, McMaster University
Hamilton, Ontario L8S 4M1 (Canada)

[**] This work was supported by NSERC (Canada), CFI (Canada) and FCAR (Quebec). The authors gratefully acknowledge Prof. M. J. Damha and his laboratory, McGill University, for helpful discussion.
Supporting information for this article is available on the WWW under http://www.angewandte.com or from the author.